

Signature of dynamical localization in the resonance width distribution of wave-chaotic dielectric cavities

Oleg A. Starykh,¹ Philippe R. J. Jacquod,¹ Evgenii E. Narimanov,² and A. Douglas Stone¹

¹*Department of Applied Physics, P.O. Box 208284, Yale University, New Haven, Connecticut 06520-8284*

²*Bell Laboratories–Lucent Technologies, 700 Mountain Avenue, Murray Hill, New Jersey 07974*

(Received 23 December 1999)

We consider the effect of dynamical localization on the widths of the resonances in open wave-chaotic dielectric cavities. We show that dynamical localization leads to a log-normal distribution of the resonance widths which scales with the localization length in excellent agreement with the results of numerical calculations for open rough microcavities.

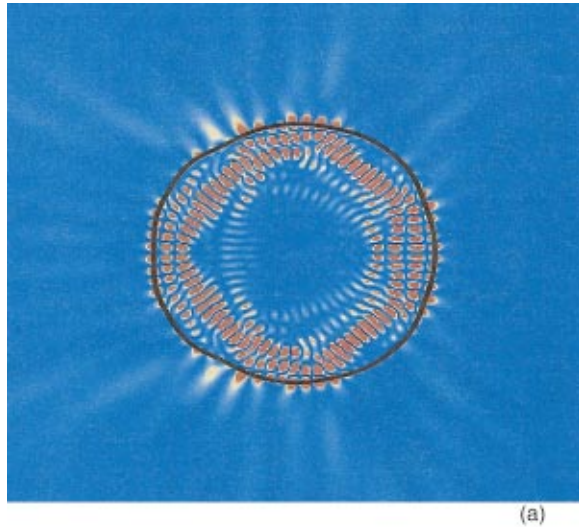
PACS number(s): 05.45.Mt, 42.55.Sa, 42.25.-p

The study of width distributions of finite quantum systems weakly coupled to a continuum is a subject of active experimental and theoretical investigation. The nature of the spectrum of resonances depends strongly on the nature of the states of the finite system “in isolation.” For example, if those states are ergodically extended and structureless over the system then the resonances will show the behavior expected from random matrix theory, the famous Porter-Thomas distribution in the case of a single channel [1]. A close relative of this resonance distribution has been measured in quantum dots in the Coulomb blockade regime [2,3]. More recently it has been pointed out that optical cavities with partially or fully chaotic ray dynamics would have interesting resonance properties and efforts have been made to characterize their distribution in various limits [4–6]. In a geometry that is approximately translationally invariant in one direction the wave equation becomes a scalar equation with a close formal analogy to the Schrödinger equation and the physics of the resonance spectrum becomes essentially the same for the optical and quantum systems. We will henceforth consider cylindrical dielectric resonators that are translationally invariant along their axis, but can be deformed in their cross section. The analog of the classical limit of the Schrödinger equation is the limit of ray optics when the wavelength of the electromagnetic field is much shorter than the typical radius of the cavity, $\lambda \ll R_0$. We will regularly use the term “quantum” to describe properties of the wave solutions that differ from the behavior of rays in the same geometry. The motion of a light ray within the cavity is identical to that of a point mass in a classical billiard and the resulting bound states are the analog of the eigenstates of “quantum billiards” [7]. However, unless the index of refraction, n , is taken infinite, none of these states are truly bound, there always being some nonzero probability of escape from the cavity. Moreover, in the case of a simple dielectric cavity the escape probability is strongly dependent on the angle of incidence of the ray. In particular, rays bouncing at the cavity’s boundary with an angle of incidence χ smaller than the critical angle $\chi_c = \sin^{-1}(1/n)$ (angles of incidence are defined from the normal to the boundary) are transmitted by refraction with high probability, while those with $\chi > \chi_c$ are trapped by total internal reflection, and can escape only with low probability by tunneling (evanescent leakage). Semiclassically the (dimensionless) angular mo-

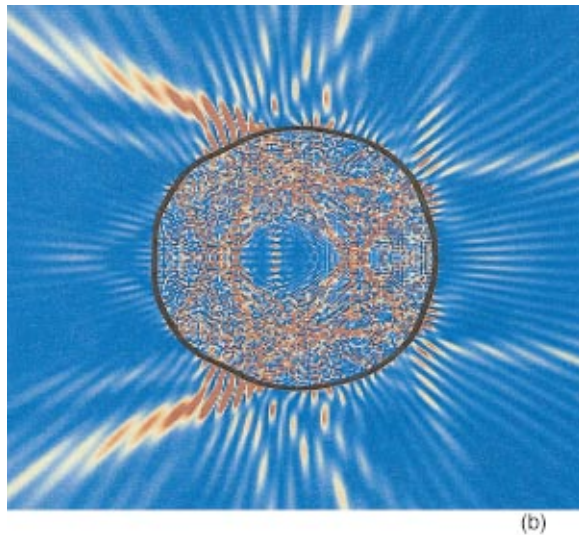
mentum of the ray in a circular cavity is $m = nkR_0 \sin \chi$, where $k = 2\pi/\lambda$ is the wave vector (in vacuum) and R_0 is the radius of the cavity. Hence a ray with angular momentum $m > kR_0$ will be strongly trapped whereas one with $m < kR_0$ will rapidly escape. Correspondingly, resonant states with mean values $\langle m \rangle > kR_0$ will have small widths, whereas those with mean values less than kR_0 will have large widths, i.e., there is a threshold value $m_c = kR_0$ for strong escape in *angular momentum space*. In an undeformed (circular) cavity m is an integral of motion and there are many exponentially long-lived “whispering gallery” resonances with $m > kR_0$.

For a generically deformed cavity angular momentum is not conserved, nor is there any other second constant of motion beyond the energy [8]. Hence the angular momentum can fluctuate. The scale of those fluctuations depends on the existence of Kolmogorov-Arnol’d-Moser tori in phase space, which limit the diffusion in angle of incidence. Beyond some critical value of the deformation these barriers are destroyed and classical rays with initial angular momenta m much larger than m_c can now diffuse to arbitrarily low angular momentum and escape by refraction [4]. As a result, even for $kR_0 \gg 1$ the width Γ_m of rays starting with $m > m_c$ is not exponentially small, and it can be estimated from the distance to the critical value in angular momentum space: $\Gamma_m = D/(m - m_c)^2$. (Here D is the effective diffusion coefficient in phase space, which in principle can depend on m .) One might then guess that a cavity with such chaotic ray dynamics will no longer support any high- Q resonances. However, this is not necessarily the case, due to the phenomenon of “dynamical localization” [9]. It is now well known that, just as a random system exhibits exponential localization in real space due to Anderson localization, the same kind of destructive interference can occur in a chaotic dynamical system and suppress diffusion in the relevant phase space [10].

The condition for the onset of dynamical localization is that the diffusion time across the system be longer than the Heisenberg time defined by the inverse level spacing of the cavity: $t_H \sim \hbar \Delta^{-1}$. For longer times than t_H , a wave packet starts to “resolve” the discreteness of the spectrum and the spreading in angular momentum is suppressed. Based on an analogy with the kicked rotator [11], the localization length ξ is determined by the classical diffusion rate D , $\xi \sim D$. Con-



(a)



(b)

FIG. 1. (Color) (a) Intensity plot of a resonance with $nkR_0 = 50$ in the rough cavity with $\kappa=0.08$, $M=15$, and $n=2.5$. Red color corresponds to the maximum of the intensity, and blue to the minimum. (b) Intensity plot of a resonance with $nkR_0 = 150$ for the same set of parameters as above.

consider a state centered around an angular momentum m_0 such that $m_0 - m_c \leq \xi$. In this case wave packets can escape before their diffusion ceases and the classical picture is adequate. Two different statistical behaviors are possible in this regime. If the escape is determined by *slow* diffusion to a boundary where escape can occur, the level width statistics has been studied recently by several authors [12–14] and they find characteristic power-law distributions. Here the diffusion constant satisfies $L \ll D \leq L^2$, and it takes many collisions to cross the available phase space (for the optical cavities the role of the system size L is played by $2nkR_0$, the number of angular momentum states available). When the diffusion constant is larger, $D \sim L^2$, the motion is ballistic in the sense that the phase space is crossed in a few collisions; this situation leads to the Porter-Thomas distribution of resonance widths and the related distributions mentioned above [1,2,15,16]. However when dynamical localization dominates then the lifetime of a localized state centered around angular momentum m_0 such that $m_0 - m_c \gg \xi$ becomes expo-

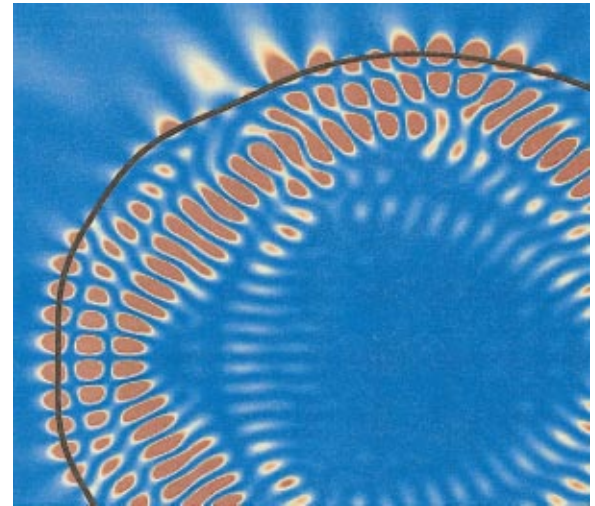


FIG. 2. (Color) Details of the wave intensity corresponding to the top resonance shown in Fig. 1. The intricate structure of the wave intensity is due to classically chaotic boundary scattering and makes the resonance clearly different from a standard whispering-gallery-like high- Q resonance.

nentially longer than the corresponding classical diffusion time to the classical emission threshold. Thus one has the possibility of high- Q resonances of completely nonclassical, pseudorandom character, something not considered in the optics literature to our knowledge (except in a very recent experiment in the microwave regime [17]). It therefore becomes of interest to understand the statistical distribution of resonance widths in such a situation.

In the localized regime $\xi/L \ll 1$, the angular momentum components of wave functions decay exponentially away from their centers and one naturally expects exponentially small average widths for states centered far above the classical emission threshold $m_0 - m_c > \xi$. Recently Nöckel and Stone [4] compared the exact lifetimes of resonances of quadrupole-deformed microcavities with the mean classical diffusion time and found the lifetimes to be significantly longer in certain cases; they conjectured that these discrepancies arose from incipient dynamical localization. Indeed, dynamical localization has been shown to occur in certain closed cavities [19,11], and a very recent experimental paper confirmed this phenomenon in microwave cavities of similar shape to those studied below [17]. However, no detailed study has been made of the statistical and scaling properties of the resonance (eigenmode) widths in this regime. These are the main topics of the current work. Below we will show that the dynamically localized regime is characterized by a very broad (log-normal) width distribution with scaling properties directly related to the system's localization length ξ . We stress that the resonance width distribution that we study here is different from the survival probability that was studied recently in the dynamically localized regime of a classically chaotic open dynamical system [18]. The survival probability, which is defined as the time it takes a state with well defined initial angular momentum (and thus not an eigenstate of the rough cavity) to escape outside, is determined by the quantum-mechanical evolution of a state with a given initial angular momentum over true resonances of the open system, each of which has a finite width. Assuming that in the local-

ized regime the resonance width is exponentially small for resonances located far away from the absorbing boundary, the survival probability is found to decay as $1/t$ for long times t [18]. These results are consistent with ours below, as we find explicitly an exponential variation of the width with the distance from the escape threshold [see Eq. (11)], but involve a different quantity, measured in a different kind of experiment.

First, to illustrate the effect of dynamical localization on the physical properties of the modes in the open cavity, we show in Fig. 1 the real-space structure of two modes of a deformed cylindrical microcavity defined according to the model described immediately below. The two modes correspond to exactly the same shape of the cavity, corresponding to fully ergodic classical ray dynamics, have the same average angular momentum $\langle m^2 \rangle^{1/2} \approx 0.5nkR_0$, but differ in their wave vector, and as a consequence (see below) differ in their localization lengths. As a result one resonance is in the quantum diffusive regime and the other in the localized regime. The qualitative difference is immediately apparent; the diffusive mode emits much more strongly and has a denser spatial structure due to the large angular momentum spread in the state. The localized mode, on the other hand, emits weakly and appears to have a caustic similar to a regular whispering gallery mode, but a closer look at its spatial structure shows that the pattern of nodes has an irregular character entirely different from the usual whispering gallery modes of circular resonators, as can be seen in Fig. 2.

We now define the model corresponding to Figs. 1 and 2. We consider an optically inactive, cylindrical microcavity with an index of refraction $n > 1$. The cross section perpendicular to the cylinder's axis is given by a circle perturbed by M harmonics of random amplitude $-1/\ell \leq a_\ell \leq 1/\ell$, $R(\phi) = R_0[1 + \sum_{\ell=2}^M a_\ell \cos(\ell\phi)]$. The average roughness of the surface is defined as $\bar{\kappa} = \sqrt{\langle \kappa^2(\phi) \rangle_\phi}$, $\kappa(\phi) = (dR/d\phi)/R_0$. This model was introduced by Frahm and Shepelyansky [11] with the condition of perfectly reflecting walls, and they referred to it as the *rough* billiard to contrast with the smoother quadrupolar deformations considered by Nöckel and Stone [4]. However, the spatial wavelength of the roughness is still assumed to be large compared to the wavelength of the resonance. The advantage of a rough boundary is that the transition to classical chaos is achieved with much smaller amplitude of deformation making it easier to explore the parameter regime of fully chaotic classical motion and dynamically localized “quantum” behavior. As we shall see below, the open rough billiard has scaling and statistical properties essentially identical to those of a quasi-one-dimensional disordered system, whereas the quadrupole billiard does not. For the rough billiard the classical dynamics can be well approximated by a discrete map for which Chirikov's overlap criterion [20] gives an estimate of the critical roughness $\bar{\kappa}_c$ above which the classical dynamics becomes fully chaotic as $\bar{\kappa}_c \sim M^{-5/2}$. The two deformation parameters M and $\bar{\kappa}$ allow one to reach a classically fully ergodic regime characterized by a diffusion constant (averaged over angular momentum) $D = \frac{4}{3}(\bar{\kappa}nkR_0)^2$ for $\bar{\kappa} \gg \bar{\kappa}_c$ and, quantum-mechanically, one gets a localization length $\xi \sim D$ [9] so that the dynamically localized regime is determined by $\bar{\kappa}^2nkR_0 \ll 1$ [11]. Keeping parameters of the cavity fixed and varying kR_0 one is able to

access states with greatly different localization lengths.

We restrict ourselves to the simplest case of a TM-polarized electric field $E(\mathbf{r})$ parallel to the cylinder axis for which both the field and its derivative are continuous at the cavity's boundary. This restriction is primarily for convenience; the TE modes obey a slightly different scalar equation which can be treated in a similar manner. It should be mentioned, however, that semiconductor quantum cascade microcylinder lasers studied in [5] emit solely in the TM mode due to a selection rule. Maxwell's equations reduce then to a single scalar wave equation, $c^{-2}\partial_t^2 E(\mathbf{r},t) = n^2(\mathbf{r},\phi)\nabla_r^2 E(\mathbf{r},t)$, where the refraction index satisfies $n(\mathbf{r}) = n$ inside the cavity, and $n(\mathbf{r}) = 1$ outside.

We use the approach in which the resonances widths in wave vector are given by the imaginary part of the wave vector of the *quasibound* states defined by the following matching conditions. First we expand the electric field in the angular momentum basis ($r \equiv |\mathbf{r}|$),

$$E(\mathbf{r},t) = e^{-ickt} \sum_{m=-\infty}^{\infty} i^m A_m(kr) e^{im\phi}, \quad (1)$$

where

$$A_m = \begin{cases} \alpha_m H_m^+(nkr) + \beta_m H_m^-(nkr) & \text{if } r \leq R(\phi) \\ \gamma_m H_m^+(kr) & \text{otherwise.} \end{cases} \quad (2)$$

This expansion corresponds to the so-called Siegert boundary conditions [21] in which the states have only an *outgoing* component at infinity [$H_m^\pm(x)$ are Hankel functions of the first and second type, respectively]. Such boundary conditions cannot be satisfied for real k and are only satisfied for discrete complex k . It can be shown that the imaginary parts of the k values that satisfy Eq. (2) are the poles of the true unitary (on-shell) S matrix of the scattering problem. From the expansion coefficients in Eq. (2) we define vectors $\boldsymbol{\alpha}$, $\boldsymbol{\beta}$, and $\boldsymbol{\gamma}$. The fields inside and outside the cavity are related by the continuity of the field and its derivative on the boundary and (after integration around the boundary) one of these equations can be used to eliminate $\boldsymbol{\gamma}$, leaving a linear relation between $\boldsymbol{\alpha}$ and $\boldsymbol{\beta}$. The matrix expressing this relation we call \tilde{S} . Moreover, the regularity of the field at the origin $r=0$ implies $\boldsymbol{\alpha} = \boldsymbol{\beta}$, and thus a secular equation for the resonant values of k is obtained of the form

$$\tilde{S}\boldsymbol{\alpha} = \boldsymbol{\alpha}. \quad (3)$$

We use the notation “ \tilde{S} matrix” because in the case of a closed billiard the matrix so defined is actually the unitary S matrix of the scattering problem of a wave incident outside the impenetrable billiard [22,23]. In our case the matrix so defined is nonunitary for any $n < \infty$ and for real k the eigenvalues of \tilde{S} have the form $\lambda_r = \exp[i(\varphi_r + i\delta_r)]$, where both φ_r and $\delta_r > 0$ are real functions of momentum k . The subscript r numbers states in a deformed cavity where angular momentum is not conserved. Exact quantization of the cavity—solving Eq. (3) exactly—implies $\lambda_r = 1$, so that the exact implementation of this procedure requires finding a complex $k = q - i\gamma$ such that $\varphi_r(q - i\gamma) = \delta_r(q - i\gamma) = 0$. The corresponding resonance width Γ_r is then given by c times γ via

the dispersion relation $\Gamma_r = c\gamma$. However, approximate widths can be found by a much more efficient procedure which is extremely helpful if one wishes to study full distributions, as we do here. First, it is straightforward to show [24] that when γ is small, simply finding the complex eigenphases $\lambda_r = \exp[i(\varphi_r + i\delta_r)]$ for real k determines the imaginary part of k on resonance by the relation $\gamma = -\delta/\varphi'$ where φ' is the derivative of the real part of the phase with respect to momentum for real k . Moreover, since this derivative can be shown to be slowly varying on the scale of the level spacing Δk , it is not necessary even to quantize the real part of the phase [i.e., to find the real k that makes $\varphi(k) = 2\pi \times \text{integer}$]. The function φ' can be easily calculated for the circular cylinder, and this relation and the assumption of slow variation of the derivative can be confirmed explicitly (for the case where γ is small). Therefore we can generate large ensembles of widths simply by diagonalizing the matrix \tilde{S} for real k and extracting the imaginary phase δ , by which means we generate $\sim 2nkR_0$ widths per diagonalization. This procedure is motivated by the work of Doron and Frischat, who noted that the statistical properties of closed billiards changed little away from the exact quantization condition (in their case it was the distribution of splittings of semiclassically degenerate states) [25]. The linear relation between δ_r and γ_r has been independently proposed earlier by Hackenbroich [26] and demonstrated for the case of the circle.

To best relate the localization properties of the eigenstates, which apply to a closed cavity, to the distribution of widths in an open cavity, we employ a perturbative formalism that was recently developed specifically to treat open optical resonators [6] (it is similar in spirit to well-known quantum perturbative scattering approaches such as R -matrix theory in the single-level approximation). According to that theory narrow resonance widths $\Gamma \ll \Delta$ (Δ is the resonance spacing) can be computed from the expectation value of an anti-Hermitian operator V taken over eigenstates $|\alpha^{(0)}\rangle$ of the matrix \mathcal{M} , which describes some effective ‘‘closed cavity,’’

$$\Gamma = b_0 \langle \alpha^{(0)} | V | \alpha^{(0)} \rangle = b_0 \sum_{m,m'} \alpha_m^{(0)*} V_{mm'} \alpha_{m'}^{(0)}. \quad (4)$$

Explicitly,

$$\mathcal{M} = (J'J') - (1/n)(J'H^+)(H^-H^+)^{-1}(H^-J). \quad (5)$$

V is the anti-Hermitian part of \mathcal{M} , and the matrix elements $(\bar{Z}Z)$ are defined as

$$(\bar{Z}Z)_{\ell m} = \frac{i^{m-\ell}}{2\pi} \int d\phi \bar{Z}_{\ell}(k) Z_m(k) e^{i(m-\ell)\phi}, \quad (6)$$

where $Z_m(k)$ and $\bar{Z}_m(k)$ stand for either $H_m^{\pm}(kR(\phi))$, the Bessel function $J_m(nkR(\phi))$, or their derivatives. The coefficient b_0 in Eq. (4) depends only on the Hermitian part \mathcal{H}_0 of \mathcal{M} , i.e., it is determined by the properties of the ‘‘closed system,’’ $b_0^{-1} = \langle \alpha^{(0)} | \partial \mathcal{H}_0 / \partial k | \alpha^{(0)} \rangle \approx \sum_m \alpha_m^{(0)*} (J'J'')_{mm} \alpha_m^{(0)}$, and can be regarded as a normalization factor. An eigenstate localized at angular momentum $m_0 \gg m_c \approx kR_0$ will have exponentially small width Γ . There-

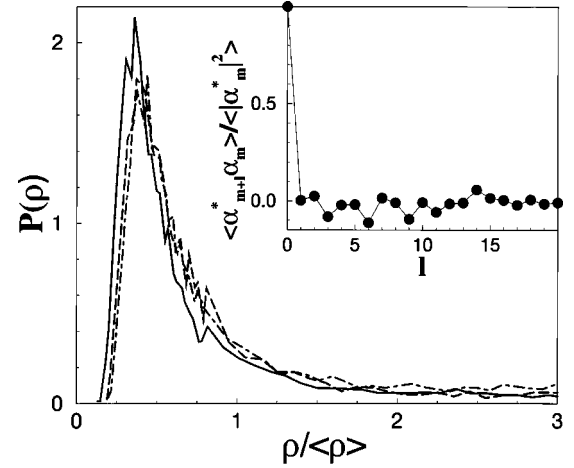


FIG. 3. Distribution of the inverse participation ratio ρ for $n = 3$, $M = 15$, and $(nkR_0, \bar{\kappa}) = (150, 0.02)$ (solid line), $(100, 0.03)$ (dashed line), and $(50, 0.06)$ (long-dashed line). $\bar{\kappa}nkR$ has been kept constant, which results in a stable average IPR $\langle \rho \rangle = 0.1 \pm 0.01$. Inset: Normalized correlation function Eq. (8) for $nkR_0 = 100$ and $\bar{\kappa} = 0.03$.

fore, for such a resonance in the semiclassical limit $\Gamma \ll \Delta$, and Eq. (4) is appropriate. More details of this formalism can be found in [6].

For an exponentially localized state one generally has

$$|\alpha_m| \sim \exp\left(-\frac{|m-m_0|}{2\xi}\right). \quad (7)$$

We consider the regime of large localization length $\xi \sim \bar{\kappa}^2 k^2 R_0^2 \gg 1$. Since the rough billiard is classically chaotic, the *phases* of the coefficients α_m change rapidly with the angular momentum, and it is natural to assume that its correlation function satisfies

$$\langle \alpha_{\ell+m}^* \alpha_{\ell} \rangle_{\ell} = \delta_{m,0} \langle |\alpha_{\ell}|^2 \rangle_{\ell}, \quad (8)$$

where the average is performed over an angular momentum interval $\ell \in [m_0 - \delta\ell/2, m_0 + \delta\ell/2]$ such that $1 \ll \delta\ell < \xi$. This behavior is illustrated in the inset to Fig. 3 for one typical set of cavity parameters, corroborating the validity of the assumption (8).

As follows from Eq. (6) and the definition of V , the matrix elements $V_{mm'}$ in angular momentum representation vary on a scale of $\delta m \sim \bar{\kappa}kR_0 \gg 1$, and therefore we can replace the product $\alpha_m^* \alpha_{m'}$ in Eq. (4) by its average value $\langle \alpha_m^* \alpha_{m'} \rangle$ over the interval $|m-m'| \sim \bar{\kappa}kR_0$. Together with Eq. (8) this leads to the diagonal approximation

$$\langle \alpha_0 | V | \alpha_0 \rangle \approx \sum_{|m|=kR_0}^{nkR_0} |\alpha_m|^2 V_{mm}. \quad (9)$$

The matrix element

$$V_{mm} = -\frac{1}{2n} [(J'H^+)_{m\ell} (H^-H^+)^{-1}_{\ell\ell'} (H^-J)_{\ell'm} - \text{c.c.}] \quad (10)$$

includes both the refractive (classical) escape from the resonator (for $|\ell|, |\ell'| < m_c = kR_0$) and the ‘‘tunneling escape’’ (corresponding to evanescent leakage [4], for $|\ell|, |\ell'| > m_c$). To evaluate the sum over angular momenta we use the stationary-phase-based technique developed in [27] in the context of the calculation of level splittings in a rough billiard. The ‘‘classical’’ refraction contribution is found to be

$$\Gamma_{m_0 > m_c}^{\text{class}} \approx \frac{k^2 R_0}{n \xi} \exp\left(-\frac{m_0 - kR_0}{\xi}\right). \quad (11)$$

This result shows that an exponentially small width can be due to the exponentially small wave function component leaking outside the classically totally-internally-reflected region. To see if this process controls the lifetime we need to compare this result with the direct ‘‘tunneling escape’’ contribution to the lifetime. The latter process involves angular momenta only above emission threshold m_c . For an estimate, it is then sufficient to evaluate the linewidth of the state above m_c in the circular cavity, which can be thought of as a state with zero localization length. We find that the tunneling contribution is also exponentially small ($n \gg 1$),

$$\begin{aligned} \Gamma_{m_0 > m_c}^{\text{tunn}} &= -(1/n) \text{Im}[H_{m_0-1}^+(kR_0)/H_{m_0}^+(kR_0)] \\ &\approx \exp[2\sqrt{m_0^2 - m_c^2} + 2m_0 \ln(m_c) \\ &\quad - 2m_0 \ln(m_0 + \sqrt{m_0^2 - m_c^2})]. \end{aligned} \quad (12)$$

Competition between the classical escape [Eq. (11)] and the tunneling [Eq. (12)] is strongest for $(m_0 - m_c)/m_c \ll 1$, i.e., when the width of the tunneling barrier is smallest. Comparing the two contributions in this region we find that $\Gamma^{\text{class}} \gg \Gamma^{\text{tunn}}$ for $\xi \gg \sqrt{kR_0}$, and $\Gamma^{\text{tunn}} \gg \Gamma^{\text{class}}$ in the opposite limit. Restriction on the range of ξ weakens as one moves to higher angular momentum, and for $(m_0 - m_c)/m_c \sim 1$ the classical escape mechanism always dominates over the tunneling one. The tunneling escape, therefore, is relevant only for very small deformations $\kappa \ll (kR_0)^{-3/4}$, which produce short localization length. Thus, the width of the states with very short (essentially zero) localization length is determined by the tunneling escape, but that of the more extended states with $\xi \gg 1$ by the classical emission from their exponentially weak tails at $m_c = kR_0$.

Having established a relation between the width and the localization length of a corresponding closed cavity, the distribution of widths then follows from the distribution of localization lengths. In one-dimensional (1D) and quasi-one-dimensional disordered systems it is now well established that the distribution of the inverse localization length is typically normally distributed around an average $1/\xi_0$ [28]. Moreover Frahm and Shepelyansky have explicitly shown [11] that the problem of the rough billiard maps onto a variant of the kicked rotor problem and hence to an ensemble of band random matrices (BRM) [30], which also describe quasi-1D disordered systems. Here the angular momentum index plays the role of the site coordinates in disordered systems, with an ideal lead (the continuum) accessible at $m_c = kR_0$. Collisions with the rough boundary correspond to random hopping between sites, which are at most $\bar{\kappa}nkR_0$ lattice spacings apart [11]. Once the critical angular momen-

tum, corresponding to the classical emission border m_c , is reached, the wave packet escapes the system and never returns. Hence we may assume that the inverse localization length in our problem has an approximately normal distribution around its mean (our ensemble here is of boundary realizations),

$$P(\xi) \sim \exp\left(-\frac{(1/\xi - 1/\xi_0)^2}{2\sigma^2}\right). \quad (13)$$

Therefore, as follows from Eqs. (11) and (13), the resonance width is distributed log-normally [31],

$$P(\Gamma) d[\ln(\Gamma)] \sim \exp\left(-\frac{\ln^2(\Gamma/\Gamma_0)}{2\sigma^2(m_0 - kR_0)^2}\right) d[\ln(\Gamma)], \quad (14)$$

where

$$\ln(\Gamma_0) = -(m_0 - kR_0)/\xi_0 \quad (15)$$

and the derivation is done in a leading logarithm approximation, so that the preexponential factor in Eq. (11) is neglected. This result is then very natural: the distribution of widths in open dynamically localized cavities is log-normal for the resonances localized far from the classical emission threshold $m_0 \gg kR_0$. This is entirely analogous to the conductance distribution of localized chains, which will be log-normal for a fixed distance from the ends [28] (see [29] for a log-normal distribution of delay times/resonance widths). We note that the relationship between dynamical localization and Anderson localization was first placed on firm footing in a seminal paper by Fishman, Grepel, and Prange [10].

Equation (14) essentially relies on two assumptions: first, Eq. (8) that the phases of the wave function components are randomly distributed with no long-range correlations, and, second, that the eigenstates are exponentially localized with a normal distribution of localization lengths. We now test the validity of these two assumptions for our rough microcavities. The validity of Eq. (8) is confirmed by the sharp drop of the correlation function $\langle \alpha_{\ell+m}^* \alpha_{\ell'} \rangle / \langle |\alpha_{\ell'}|^2 \rangle$ for $m > 0$, which is clearly seen from the numerical results presented in the inset to Fig. 3. The localization properties are investigated by computing the distribution of the inverse participation ratio (IPR) defined as $\rho = \sum_m |\alpha_m|^4 / \sum_m |\alpha_m|^2$. The IPR measures the inverse number of effective eigenstate components and thus allows one to distinguish between localized and delocalized states. Generally, in the localized phase $\langle \rho \rangle$ is independent of the system size since at most $\xi \ll L$ sites contribute to the sum and $\langle \rho \rangle \sim \xi^{-1}$. In the other limit of ergodic states, all sites contribute equally and $\langle \rho \rangle \sim L^{-1}$ in this case. Between these two limits, a variety of behaviors may occur depending on the inner structure of the eigenstates. In Fig. 3 we show IPR distributions for three different parameter sets corresponding to the same average localization length $\xi \sim (\bar{\kappa}nkR_0)^2 \equiv 9$. The three distributions are indeed stable under parameter variations when ξ is kept constant, and this shows that not only the average IPR/localization length [11] but also the full IPR distribution obey a one-parameter scaling with $\bar{\kappa}nkR$. The situation is very similar to the one studied in Ref. [30] for BRM with a

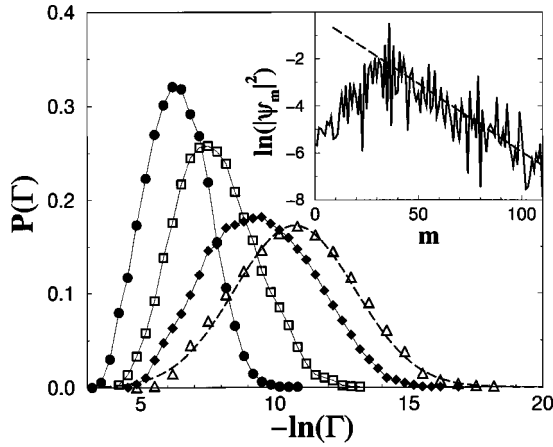


FIG. 4. Distribution of resonance widths for $n=3.5$, $nkR \approx 110$, $\bar{\kappa}=0.018$, and $M=15$ for states with average angular momentum $m_0/(nkR_0)=0.5$ (circles), 0.6 (squares), 0.7 (diamonds), and 0.8 (triangles). This last distribution is fitted according to Eq. (14) with $\sigma \approx 0.04$ (dashed line). The emission border is at $m_c \approx 0.29nkR$. Each distribution is constructed from 8000 to 13000 widths obtained from 1013 boundary realizations of the rough cavity. Inset: Typical localized eigenstate for the same parameter set. The dashed line indicates an exponential decay corresponding to a localization length of $\xi=16$.

bandwidth $1 \ll b \approx \sqrt{2\xi}$, for which the IPR distribution was analytically computed. Similar deviations as those seen on Fig. 3 are also present for BRM with not too large bandwidths [30], so that these numerical results confirm the universality of the dynamically localized regime, quite analogous to quasi-one-dimensional disordered systems. We also illustrate this exponential localization by showing one typical state in the inset to Fig. 4.

Having tested the validity of the main assumptions on which Eq. (14) relies, we present in Fig. 4 the distribution of widths for the classically chaotic, dynamically localized regime of the open rough microcavity. The distributions shown correspond to resonances centered in intervals of width $\delta m/(nkR_0)=0.1$ around angular momenta $m_0/(nkR_0)=0.5, 0.6, 0.7$, and 0.8 , well above the classical threshold $m_c/(nkR_0) \approx 0.29$. Clearly, the distributions are log-normal and their widths increase as one moves away from the classical emission border $m_c = kR_0$. Furthermore, the agreement with Eq. (14) is quantitatively confirmed by a direct fit of the broadest of these distributions (see dashed line on Fig. 4).

We expect by analogy to the scaling theory of localization that the logarithmic average of the widths will exhibit a universal scaling behavior. This expectation is confirmed by the data shown in Fig. 5 where we present numerical results for the scaling obeyed by $\ln \Gamma_0$. Log-averages for different parameter sets have been computed for at least 2000 widths in narrow energy windows $\delta m/(nkR_0)=0.2$ around given angular momenta $m_0 > m_c$ for different values of indices of refraction $1.5 \leq n \leq 4$, wavelengths $75 \leq nkR_0 \leq 180$, and roughnesses $\bar{\kappa}$. All presented results are in the localized regimes $\xi < m_0 - m_c$ and the corresponding curves have been put on top of each other by a one-parameter scaling. Figure 5 demonstrates the validity of the linear relation (15), as is indicated by the straight line. The exact parameter dependence of the scaling can be deduced from analogy to the

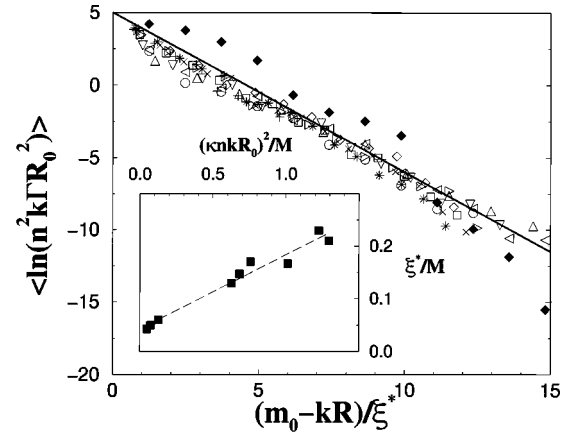


FIG. 5. Scaling of the average logarithm of resonance width $\langle \ln \Gamma_0 \rangle$ vs $(m_0 - kR)/\xi^*$ for parameters $95 < nkR < 195$, $2.5 < n < 5$, $0.008 < \bar{\kappa} < 0.03$, and $10 < M < 30$. Open symbols correspond to the rough deformation for which a one-parameter scaling exists. The full diamonds correspond to a quadrupolar billiard ($M=2$) for which the diffusion is affected by classical invariant structures in phase space. Inset: Localization length as extracted from the scaling shown on the main panel.

scaling theory of localization. In this case the Thouless conductance $g = \Gamma/\Delta\epsilon$ is the scaling quantity (or its logarithm in the localized regime); here Γ is the resonance width, and $\Delta\epsilon$ is the mean level spacing. In our case $\Gamma = c\gamma$ (where γ is the width in momentum space), but $\Delta\epsilon$ differs from the value in the corresponding Schrödinger equation, due to the different dispersion relation for the wave equation. Taking this into account one finds that the analog of the dimensionless conductance is $g \sim n^2kc\gamma R_0^2$, and it is the logarithm of this dimensionless quantity that we plot against $(m_0 - kR)/\xi^*$. Figure 5 allows us to identify the scaling parameter ξ^* with the localization length up to a free parameter. That this scaling holds for the rough cavity demonstrates that the localization length is independent of the angular momentum, as is expected for a homogeneously diffusive system. The situation is fundamentally different for a quadrupolar cavity ($M=2$) as can be seen in Fig. 5 (see black diamonds). Obviously, one scaling parameter is not sufficient to bring the corresponding curve on top of the other ones satisfying Eq. (15). This indicates an angular momentum dependent diffusion constant, which directly follows from the effective local map derived for this particular case [32]. Furthermore, in the regime corresponding to the data presented for the quadrupolar deformation, small invariant torii and islands of stability still survive, resulting in strongly localized wave functions with short localization lengths determined essentially by the size of the remaining classical structures. Because of this, and unlike the situation in the rough cavity, the width of such states is determined by the tunneling escape [see the discussion after Eq. (12)]. Therefore a clean demonstration of exponential dynamical localization is difficult in the quadrupolar billiard.

Further confirmation that the extracted scaling parameter is indeed related to the system's localization properties is given in the inset to Fig. 5 where ξ^* is plotted against the diffusion constant $D = (\bar{\kappa}nkR_0)^2$ as derived from the effective rough map [11]. This inset gives unambiguous confir-

mation of the above derived relation between localization length and log-averaged width. Note that ξ^* has a linear dependence on the diffusion constant D even at small D where the relation $\xi \sim D$ does not hold. For large D , however, the relation $\xi^* \sim \xi$ holds [33].

To summarize, we have presented a study of the width distributions of a quantum-chaotic open system in the dynamically localized regime. This study was greatly expedited by the linear relation between the complex phases of the eigenvalues of the nonunitary scattering matrix away from exact quantization and the imaginary part of the corresponding exactly quantized complex wave vector, which has allowed us to generate sufficiently large width statistics to demonstrate the log-normal form of their distribution. The width distribution has been derived analytically assuming a normal distribution of inverse localization lengths and phase randomness of the wave functions, using a recently developed semiclassical method, the usefulness of which is thus

further demonstrated [6], and confirmed numerically. The log-normal distribution is a hallmark of localized disordered systems and hence our results deepen the analogy between dynamical and Anderson localization and point out an optical observable that can in principle be measured to demonstrate this distribution. The possibility of high- Q resonances in deformed rough cavities (which are nonetheless smooth on the scale of the wavelength) should be of interest in optical studies of scattering from small particles; however, their random nature seems to make such resonances unsuitable for applications.

We have benefited from interesting discussions with F. Borgonovi, C. Texier, and Y. Fyodorov and would like to thank G. Maspero for sending us his thesis and A. D. Mirlin for communicating several interesting references. We acknowledge the support of the Swiss NSF and NSF Grant No. PHY9612200.

-
- [1] C. E. Porter and R. G. Thomas, *Phys. Rev.* **104**, 483 (1956).
 [2] R. A. Jalabert, A. D. Stone, and Y. Alhassid, *Phys. Rev. Lett.* **68**, 3468 (1992).
 [3] A. M. Chang *et al.*, *Phys. Rev. Lett.* **76**, 1695 (1996); J. A. Folk *et al.*, *ibid.* **76**, 1699 (1996).
 [4] J. U. Nöckel and A. D. Stone, *Nature (London)* **385**, 45 (1997).
 [5] C. Gmachl, F. Capasso, E. E. Narimanov, J. U. Nöckel, A. D. Stone, J. Faist, D. L. Sivco, and A. Y. Cho, *Science* **280**, 1493 (1998).
 [6] E. E. Narimanov, G. Hackenbroich, Ph. Jacquod, and A. D. Stone, *Phys. Rev. Lett.* **83**, 4991 (1999).
 [7] H. J. Stockmann and J. Stein, *Phys. Rev. Lett.* **64**, 2215 (1990).
 [8] It has been proved that only elliptical deformation of the circle does not destroy the integrability: S. Chang and R. Friedberg, *J. Math. Phys.* **29**, 7 (1988).
 [9] B. V. Chirikov, F. M. Izrailev, and D. L. Shepelyansky, *Physica D* **33**, 77 (1988).
 [10] S. Fishman, D. R. Grempel, and R. E. Prange, *Phys. Rev. Lett.* **49**, 509 (1982); see also D. L. Shepelyansky, *Physica D* **28**, 103 (1987).
 [11] K. Frahm and D. L. Shepelyansky, *Phys. Rev. Lett.* **78**, 1440 (1997); **79**, 1833 (1997).
 [12] F. Borgonovi, I. Guarneri, and D. L. Shepelyansky, *Phys. Rev. A* **43**, 4517 (1991).
 [13] G. Casati, G. Maspero, and D. L. Shepelyansky, *Phys. Rev. E* **56**, R6233 (1997); K. Frahm, *ibid.* **56**, R6237 (1997).
 [14] G. Maspero, Ph.D. thesis Università di Milano, sede di Como, 1998 (unpublished).
 [15] Y. Alhassid and C. H. Lewenkopf, *Phys. Rev. B* **55**, 7749 (1997).
 [16] Y. V. Fyodorov and H. J. Sommers, *J. Math. Phys.* **38**, 1918 (1997).
 [17] L. Sirko *et al.*, *Phys. Lett. A* **266**, 331 (2000).
 [18] G. Casati, G. Maspero, and D. Shepelyansky, *Phys. Rev. Lett.* **82**, 524 (1999).
 [19] F. Borgonovi, G. Casati, and Baowen Li, *Phys. Rev. Lett.* **77**, 4744 (1996).
 [20] B. V. Chirikov, *J. Nucl. Energy, Part C* **1**, 253 (1960).
 [21] A. F. J. Siegert, *Phys. Rev.* **56**, 750 (1939).
 [22] E. Doron and U. Smilansky, *Phys. Rev. Lett.* **68**, 1255 (1992); *Nonlinearity* **5**, 1055 (1992).
 [23] B. Dietz and U. Smilansky, *Chaos* **3**, 581 (1993).
 [24] Ph. Jacquod, E. E. Narimanov, O. A. Starykh, and A. D. Stone (unpublished).
 [25] E. Doron and S. Frischat, *Phys. Rev. Lett.* **75**, 3661 (1995).
 [26] G. Hackenbroich (unpublished).
 [27] G. Hackenbroich, E. E. Narimanov, and A. D. Stone, *Phys. Rev. E* **57**, R5 (1998).
 [28] P. W. Anderson, D. J. Thouless, E. Abrahams, and D. S. Fisher, *Phys. Rev. B* **22**, 3519 (1980).
 [29] B. L. Altshuler and V. N. Prigodin, *Zh. Éksp. Teor. Fiz.* **95**, 348 (1989) [*Sov. Phys. JETP* **68**, 198 (1989)]; C. Texier and A. Comtet, *Phys. Rev. Lett.* **82**, 4220 (1999); M. Titov and Y. V. Fyodorov, e-print cond-mat/9909010.
 [30] Y. V. Fyodorov and A. D. Mirlin, *Phys. Rev. Lett.* **67**, 2405 (1991); **71**, 412 (1993).
 [31] An exponentially large number of lifetimes is needed to construct a log-normal distribution function.
 [32] J. U. Nöckel, Ph.D. thesis, Yale University, 1997 (unpublished).
 [33] A. Mekis, J. U. Nöckel, G. Chen, A. D. Stone, and R. K. Chang, *Phys. Rev. Lett.* **75**, 2682 (1995).